Anti Vortex Device to Operate Pump Intakes Below the Minimum Submergence

M. A. Angulo
UNLP, mauricio.angulo@ing.unlp.edu.ar

A. Rivetti
UNLP

C. V. Lucino
UNLP

S. O. Liscia
UNLP

Recommended Citation

Angulo M.A., Rivetti, A., Lucino, C.V., and Liscia, S.O. (2022). "Anti Vortex Device to Operate Pump Intakes Below the Minimum Submergence" in "9th IAHR International Symposium on Hydraulic Structures (9th ISHS)". *Proceedings of the 9th IAHR International Symposium on Hydraulic Structures – 9th ISHS*, 24-27 October 2022, IIT Roorkee, Roorkee, India. Palermo, Ahmad, Crookston, and Erpicum Editors. Utah State University, Logan, Utah, USA, 9 pages (DOI: 10.26077/3fa1-7f82) (ISBN 978-1-958416-07-5).

9th International Symposium on Hydraulic Structures Roorkee, India 24-27 October 2022
ISBN 978-1-958416-07-5 DOI: https://doi.org/10.26077/3fa1-7f82

Anti vortex device to operate pump intakes below the minimum submergence

M.A. Angulo[1], A. Rivetti[1], C.V. Lucino[1] & S.O. Liscia[1]
[1]*Laboratory of Hydromechanics, UNLP, La Plata, Argentina*
E-mail: mauricio.angulo@ing.unlp.edu.ar

Abstract: *Thermal power plants require water cooling pump stations to inject fresh water into the condenser. Generally, these pump stations have vertical mixed-flow pumps with large flows and low-to-medium heads that take water from rivers or reservoirs. Under certain natural conditions, water sources can reach extraordinarily low levels, thus affecting pump operation as the minimum recommended submergence might not be met, causing the power plant to be powered off. This causes both a very high loss of profit for the company and a decrease in the available power for the electrical supply system. Therefore, expanding the range of submergence under which pumps could be operated safely for special, transitory, and emergencies is an alternative worth exploring. Pump operation below the minimum level gives rise to unacceptable vortices on the free surface, air entrainment inside the circuit, higher mechanical vibrations, and lower efficiencies due to higher pre-swirl at the suction bell. Because of this, an anti-vortex device is proposed to prevent free surface vortex formation to allow the operation of the pump over a wider range of submergence. The device has a grating shape and was designed and optimized based on scale model tests performed on a typical pump bay following the ANSI standard intake design. Flow analyses through particle image velocimetry (PIV), acoustic Doppler velocimetry (ADV) velocity profiles, and swirl-meter measurements were carried out for a range of levels under the minimum and then compared with the device installed under the same conditions. Experiments proved the effectiveness of the solution to reduce free surface vortex formation and pre-swirl, allowing pumps to operate down to half of the recommended submergence.*

Keywords: *Pump station, submergence, free surface vortex.*

1. Introduction

Large pump stations are required to provide cold water for thermoelectric power plants. Water is extracted from rivers or lakes and then pumped to the gas turbine condenser to cool vapor. As this process is critical for continuous operation, pumps should never stop. Usually, vertical mixed-flow pumps are installed at these pump stations (Kushwaha 2015), able to provide high flows at medium-to-low heads. Under certain natural conditions, water sources may cause the free surface level to descend below the guaranteed submergence. Such operating condition is not recommended as surface vortices may appear from the free surface level and grow enough to let air enter the pump sump, injecting air inside the cooling system and inducing vibrations, noise, and efficiency loss at pumps. In such cases, the pump station has to be shut down, thus affecting the electrical supply system. The power plant owner/operator has to deal with power shortage and thus loss of profit.

To operate under the minimum submergence, different solutions were evaluated. For example, deepening the pump bay locally at the pump suction bell and/or placing the pump suction at the lowest possible, but both alternatives have high civil and mechanical costs and long schedules to implement the solutions. Besides, general guidelines concerning geometry and flow characteristics of pump intake structures design, ANSI/HI 9.8 (2018) standard proposes several devices to prevent or reduce submerged vortices formation employing splitters or fillets and suggests a few devices for superficial vorticities, such as vertical or tilted curtains and horizontal gratings; Harun et al. (2020) tested a floor splitter plate that reduces floor vortices and decreases the intensity of swirling at the inlet flow; Norizan et al. (2019) studied the optimization of floor splitters while Sherestha et al. (2021) optimized the bell mouth shape to suppress vorticity at the entrance. Just a few references were found of structures designed to prevent free surface vortices formation for submergible pumps, most of them related to sumps with lateral intakes, such as the "vortex breaker", mentioned by Jones et al. (2008), a structure which consists on bars parallel to flow direction, and an angle with the free surface, and rafts located above lateral intakes and Park et al. (2018), who propose a floating anti-vortex device which consists of four legs and a floating body surrounding the intake pipe.

The problem caused by superficial vortices is also addressed at intake structures of hydropower plants, where sometimes it is necessary to install vortex suppressors designed to increase the distance between the water surface and the intake by installing, for example, a floating plate in the path of the vortex (Taghvaei 2012).

Regarding CFD simulations, Constantinescu et al. (1998) simulated a pump bay; Arocena et al. (2021) implemented simulations of the bay including the pump itself to measure the impact of vortices on the efficiency. However, as numerical simulations must capture a small enough vortices scale, meshes grow increasingly finer and, as a result, the computational costs are high when trying to simulate many scenarios combining different free surface levels and the geometry changes at the bay.

We propose an antivortex device, a floating grid (FG), that allows the operation of pumps safely under the guaranteed submergences and also below the submergences recommended on the reference code ANSI/HI 9.8. The proposed device is partially submerged and surrounds the vertical pump geometry that reduces significantly the free surface vortices type 3 to 6 reducing them to lower types 1 and 2. The tests carried out are aimed at comparing the operation of a pump station below the minimum submergence with and without the antivortex device. The pump bay design is based on standard guidelines and has no fillets, splitters, or any other geometry element to prevent vortex formation. Photographs, videos, PIV measurements, ADV profiles, and swirl-meter measurements were performed to contribute to the comparison.

2. Materials and methods

2.1. Experimental set-up

The project is based on a real-scale pump station. A physical model of one bay of the pump station was built (scale 1:11.875) and installed inside a test channel of the Laboratory of Hydraulics of the UNLP. The channel consists of a closed-loop circuit that provides the inflow of water from a constant level reservoir. The pump is simulated using a siphon pipe and the pump case geometry corresponds to the commercial vertical pump Torishima SPV 1500 with a nominal flow of 25,000 m³/h and 43.5 m head. The suction bell diameter is 2.28 m. In Figure 1, a detail of bay geometry and dimensions is shown. The prototype scale has a corner, back wall, and side wall fillets, also a center splitter to reduce sub-surface vortices. The test reported in this paper has none of these structures, as the target was to test a more general bay design.

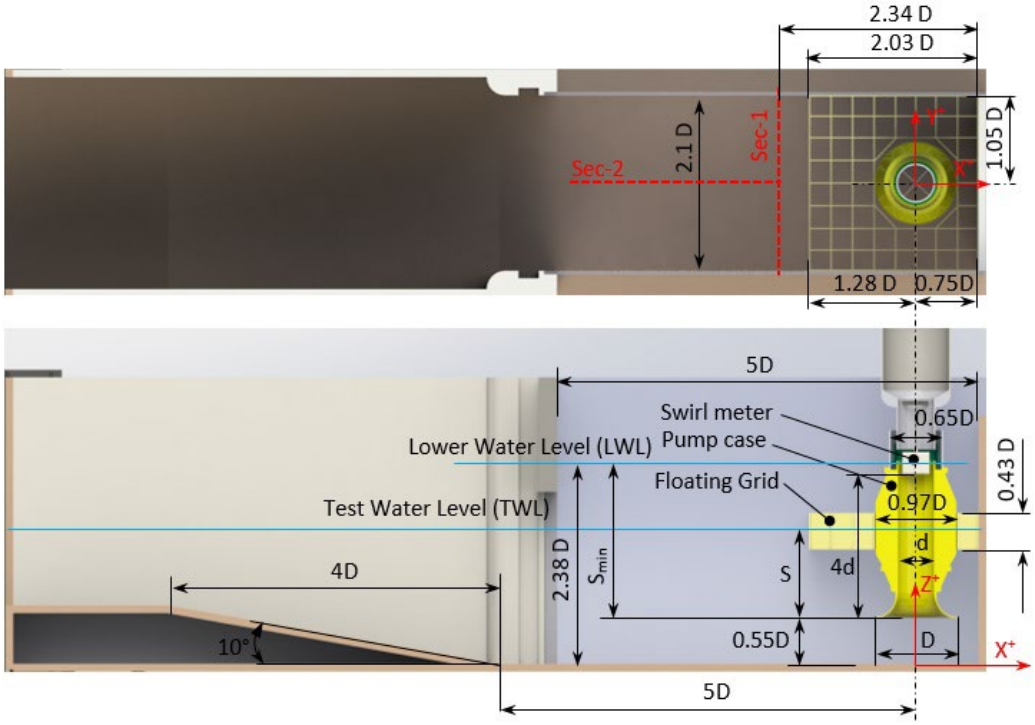

Figure 1. Plan view and cross-section of the pump bay, its dimensions are parametrized by the pump suction bell diameter (*D*). The swirl meter position is indicated in the cross-section, its diameter is 0.75*d* and the height 0.6*d*.

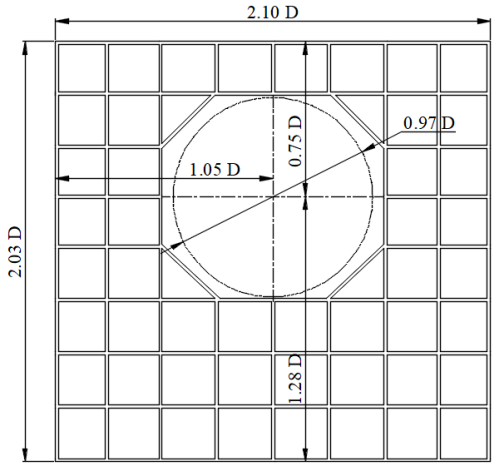

Figure 2. Plan view of the floating grid, it has 8x8 cells with a hole to avoid the pump case contact (dashed circle). The grid is orthogonal but is not uniform and should be adjusted to the pump case diameter.

Concerning the proposed antivortex device (Figure 2), the design concept is aimed at reducing the size of the free surface vortices by splitting them into higher numbers. As the available energy of each vortex decreases, so does its ability to depress the free surface. The grid is neither in contact with the pump body nor with the bay walls. It is submerged at 70 % of its height (0.3 *D*), and as it is floating, it follows the surface level permanently. The grid is orthogonal and has 8 columns by 8 rows, the cells are not of the same dimensions but the size of the sides of the squares is between 0.23 *D* and 0.27 *D*. The height is 0.43 *D* (1 m at prototype) and the grid is extended 1.28 *D* from the pump shaft axis.

The tests were done for a flow of 1.28 Q_n equal to 0.0183 m³/s (32.000 m³/h at prototype). This higher flow is under the code recommendations (ANSI/HI 9.8, section 9.8.5.3) to test the final design at 1.5 times the Froude scaled flow to increase circulation and produce stronger vortices resulting in a conservative prediction even when no scale effects are probable. The bay-free surface level is expressed by the relative submergence, *S/D*. The submergence *S/D* = 1.83 is the minimum free water level (*MWL*) at the bay recommended by the pump designer. This value is under ANSI 9.8/HI recommendations expressed by the equation [1].

$$S/D = 1 + 2.3F_D \tag{1}$$

$$F_D = \frac{V}{\sqrt{gD}} \tag{2}$$

Where *S* is the submergence, *D* is the outer diameter of the suction bell, F_D is the Froude number, *V* is the mean velocity at the suction bell, and *g* is the acceleration of gravity.

Reynolds number at the model is *Re* = 135,080 and the Weber number is *W* = 1,050; in both cases, they verified the recommended limits of *Re* > 110,000 and *W* > 720 (Odgaard 1986) to account for scale effects due to friction and surface tension.

The inlet flow at the bay was measured with an orifice plate with corner tapping following ISO 5157-2:2003 guidelines. The free surface level at the bay was measured with a vertical ruler at the entrance. The free surface fluctuation was negligible for all tests.

Table 1. Performed tests. Water levels at the bay are expressed as a ratio with the suction bell diameter and also as the ratio between the descent of water level (relative to the *LWL*) and the minimum submergence recommended by the pump designer.

S/D [-]	$(LWL\text{-}TWL)/S_{min}$ [%]	Without FG	With FG
1.83	0	1	1-FG
1.61	12	2	2-FG
1.30	29	3	3-FG
1.17	36	4	4-FG
0.95	51	5	5-FG
0.82	58	6	6-FG

In order to detect the presence of vortices at the free surface and to quantify the intensity, three approaches were implemented: the PIV measurements technique, velocity profiles with ADV measurements, and circulation estimations by means of swirl meter measurements. The ANSI 9.8/HI classification of the free surface vortices was adopted to describe vortex observations. Small Polypropylene balls were used as tracers and classify vortices between types 3 and 4 which can pull particles but not air.

It was assumed for all tests that the grid does not affect the development of subsurface vortices. Therefore, the swirl angle variations between the cases with and without a floating grid are exclusively due to its influence.

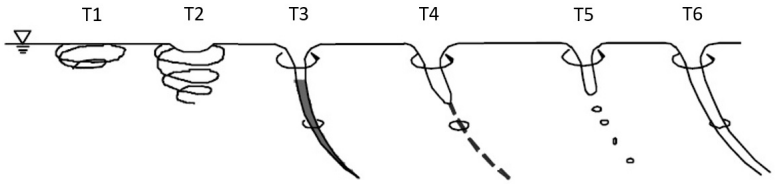

Figure 3. Classification of free vortex type according to ANSI 9.8/HI

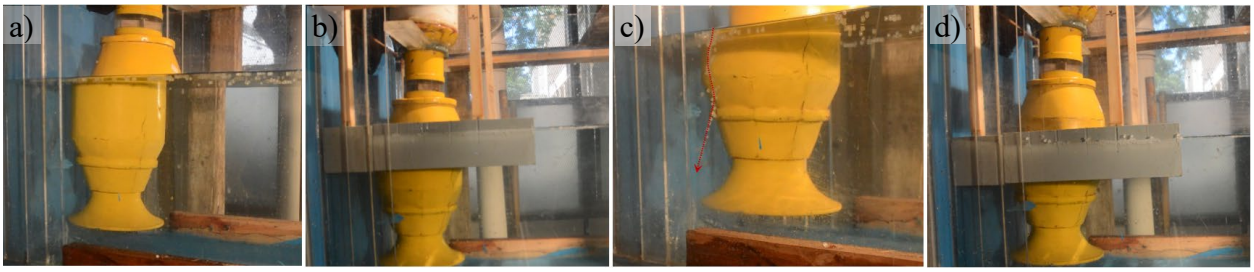

Figure 4. For a) and b) side views, *S/D* = 1.17 compared with and without FG. For c) and d) side view, *S/D* = 0.95 compared with and without FG. In c) a vortex core type 4 is pointed with a dashed line which is not visible for d).

2.2. PIV measurements

Two cameras were located above the pump bay, one in front of and the other behind the pump case, in order to obtain a zenithal view suitable to capturing the free surface vortices. Videos were recorded simultaneously and then merged in a unique frame. As the vortices occurrence is unsteady, the video is 180-second long. Small Polypropylene particles were seeded at the bay as surface flow tracers. The time lapse where vortices appeared was analyzed utilizing the PIVlab tool.

2.3. ADV measurements

Two velocity profiles were measured for all tests, one cross-section (Figure 1, Sec-1) and a longitudinal section (Figure 1, Sec-2). Each section was divided into a grid with 35 points. Measurements were made with an ADV Vectrino Plus (Nortek). 3D velocities were measured for 5 minutes at each point and industrial powder was used to increase water turbidity to get a signal-to-noise ratio, *SNR* > 15 dB, and correlation factors > 70 %. Raw data was post-processed with WinADV 2.03 (USBR) filtering spikes to guarantee good velocity profiles.

2.4. Swirl meter measurements

To measure the intensity of flow rotation in the suction pipe (θ) a swirl meter was installed following ANSI/HI 9.8 recommendations. The number of revolutions is accounted for during a lapse of 10 minutes for long-term evaluation and 30 seconds for the short term. This velocity is used to calculate de swirl angle utilizing the following equation:

$$\theta = tan^{-1}(\pi\, d\, n/u) \tag{3}$$

Where d is the diameter of the pipe at the swirl meter (83 mm), n represents the revolutions per second of the swirl meter and u is the average velocity at the swirl meter.

3. Results

3.1. Free surface velocity and vorticity (PIV)

In Figure 5, PIV results are shown in terms of instant (Ω_z) and average ($\overline{\Omega}_z$) vorticity in vertical direction Z. Without FG, average vorticity shows that superficial vortices are located around the left area of the suction pipe. Close to the pump case, vortices are negative (clockwise rotation), and close to the side wall, they are positive (counterclockwise rotation). This result is consistent with the shear wall effect in the superficial flow. The highest vortex intensity was obtained for a submergence of 0.95 *S/D.* At 0.82 *S/D*, the free surface is more stable in terms of vortex formation. In Figure 5.b, instant vorticity shows the same pattern. The frame chosen shows an individual vortex formation type IV. Figure 5.c shows the results with the FG. Average vorticity in the Z direction is not analyzed since all the values are close to zero. Instant vorticity shows vortex formation in the area located upstream of the FG. The maximum intensity is for a submergence equal to1.17 *S/D*. Inside the grid cells, no vortex formation is visible in this analysis.

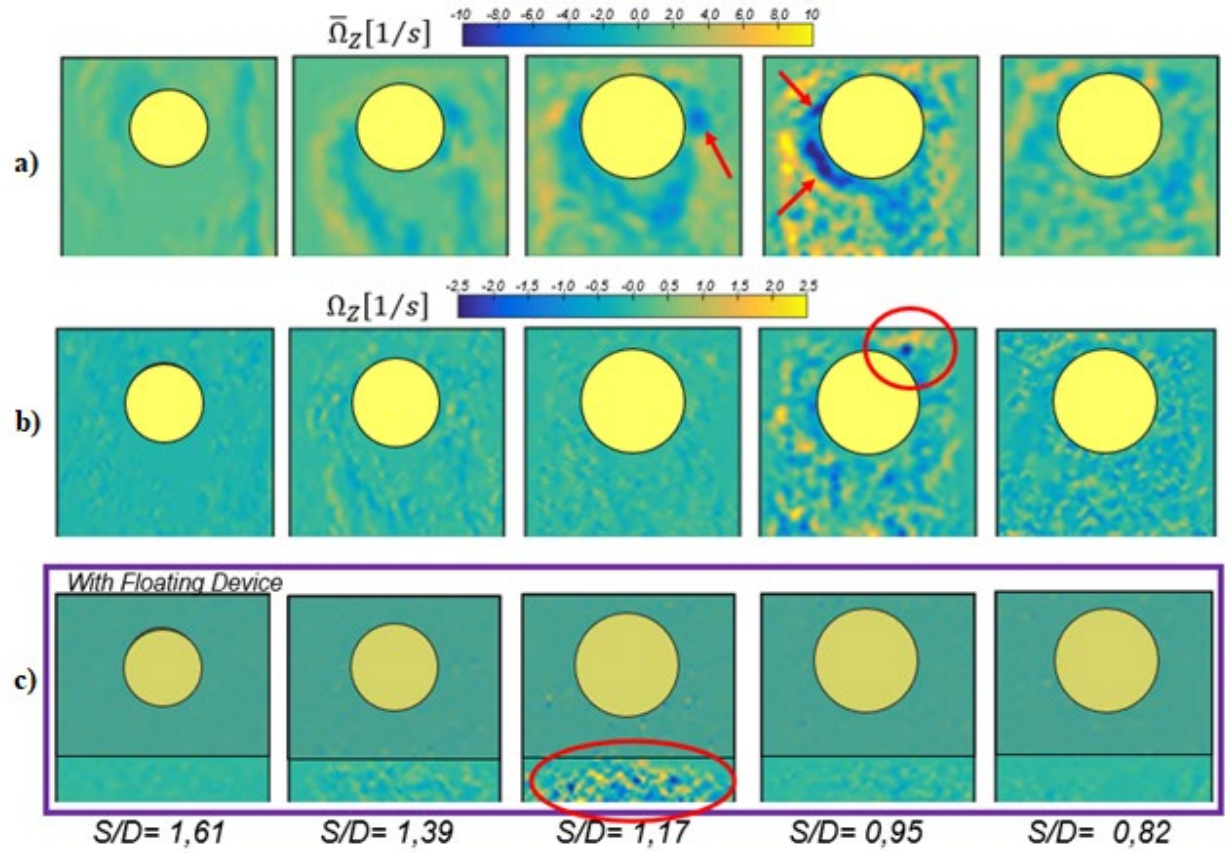

Figure 5. Free surface vorticity in the *Z* direction was obtained with PIV measurements at different submergence levels, ranging from 1.61 to 0.82 *S/D*. a) Average vorticity ($\overline{\Omega}_z$) for 2 min window. Maximum vortex development is seen at *S/D* between 1.17 and 0.95 close to the suction pipe (red arrows). b) Instant vorticity (Ω_z) frame without FG case. A free surface vortex is identified for *S/D =0.95* (red circle). c) Instant vorticity (Ω_z) frame for FG case. Vorticity inside the grid cells is almost cero. For *S/D* between 1.39 and 0.95, a random vorticity pattern is detected inside the cells (red circle).

3.2. Velocity profile upstream the pump intake (ADV)

Figures 6 and 7 show average velocity profiles and standard deviation of velocity for a window size of 300 s. For a submergence of 1.83 *S/D*, the flow distribution remains mostly undisturbed by the presence of the FG. As submergence decreases, the flow distribution appears to be more uniform and stable with the presence of the FG. Without the FG, the flow tends to concentrate more on the left side of the channel. The standard deviation of the velocity module shows that, for submergences below 1.61 *S/D*, velocity fluctuation increases between 15% to 40%.

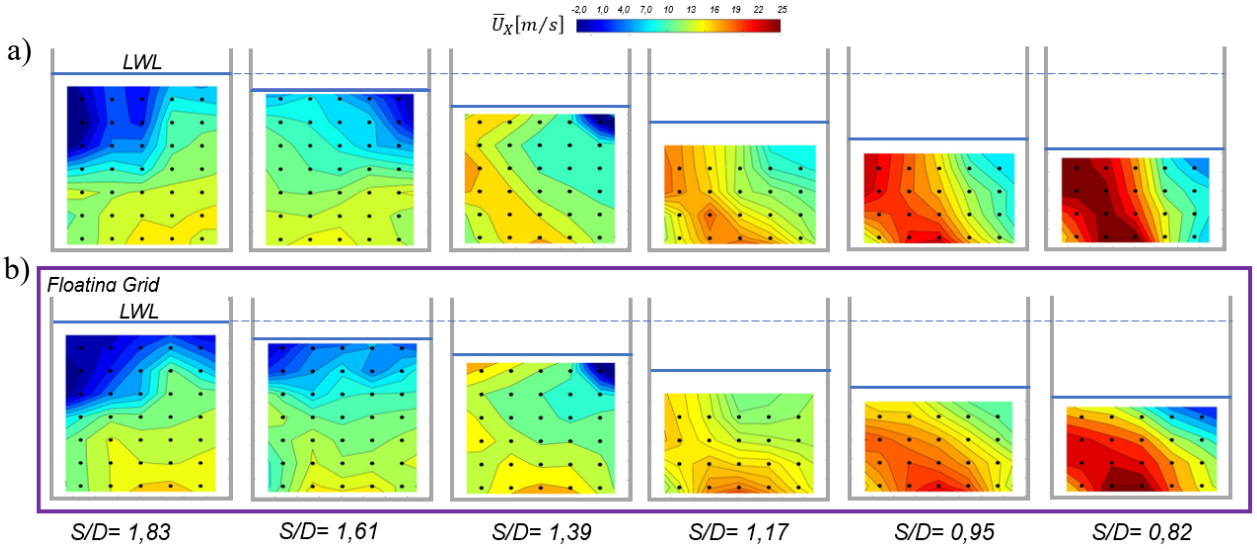

Figure 6. Average X-velocity ($\overline{U}_x$) profiles for a cross-section at a distance of 0.31D upstream of the FG. Submergence levels decrease from left to right ranging from 1.83 to 0.82 *S/D*. Measured probe's locations are indicated with black dots. a) Without FG, the flow tends to concentrate to the left for submergences below 1.39 *S/D*. b) With FG, the flow is more uniform with a small tendency to the left for submergences between 0.95 and 0.82 *S/D*.

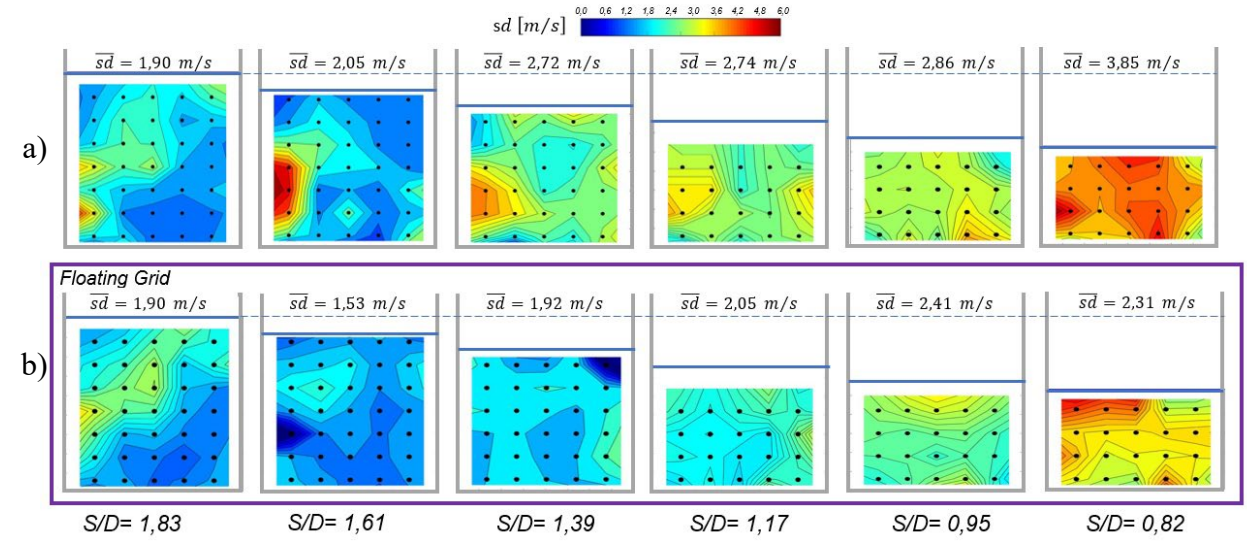

Figure 7. Standard deviation (sd) profiles of velocity module for a cross-section at a distance of 0.31D upstream of the FG. Submergence levels decrease from left to right ranging from 1.83 to 0.82 *S/D*. Measured probe's locations are indicated with black dots. a) Without FG, the flow is more unstable for smaller submergence levels. Mean deviation values decrease from 1.9 m/s to 3.85 m/s going as submergence spans from its maximum to its minimum). b) With FG, the standard deviation distribution remains more uniform as the submergence level decreases. Mean deviation values are 15% to 40% smaller as compared to a).

3.3. Swirl in the suction pipe (Swirl meter)

Table 2 and Figure 8 show the analysis of the flow rotation and the inlet of the pump. For the minimum submergence allowed by the ANSI standard, *S/D* = 1.83, the acceptance criteria of maximum rotation are achieved for both cases (with and without FG). The long-term swirl average angle is below 5° and the short-term swirl average angle is below 7° (Figure 8.a). For submergence levels below 1.39, without the FG, the acceptance criterion is no longer achieved. For *S/D* = 1.61, the swirl angle is nearly zero since the direction of rotation changes from negative to positive from

S/D = 1.83 to *S/D* = 1.39. This result is in accordance with the flow distribution analyzed in Figure 6, where the flow changes the tendency to be concentrated on the right of the channel for *S/D* = 1.83 to the left for *S/D* below 1.39. Figure 8.b shows that swirl fluctuation is larger without the FG.

Table 2. Swirl in the suction pipe, with and without the floating grid at different submergence levels.

		Swirl in the suction pipe					
Case		**S/D = 1.83**	**S/D = 1.61**	**S/D = 1.39**	**S/D = 1.17**	**S/D = 0.95**	**S/D = 0.82**
Without Flotating Grid	Long-term Swirl angle [°]	-5.2	0.4	9.1	8.5	13.1	14.3
	Short-term Swirl angle [°]	-5.9	0.4	11.2	10.8	18.8	17.9
	Swirl angle Desviation [°]	0.4	0.0	0.8	1.0	1.2	1.3
With Flotating Grid	Long-term Swirl angle [°]	0.0	1.2	1.6	2.6	3.6	6.5
	Short-term Swirl angle [°]	0.0	1.2	1.5	2.6	3.8	4.2
	Swirl angle Desviation [°]	0.0	0.1	0.6	0.2	0.4	0.8

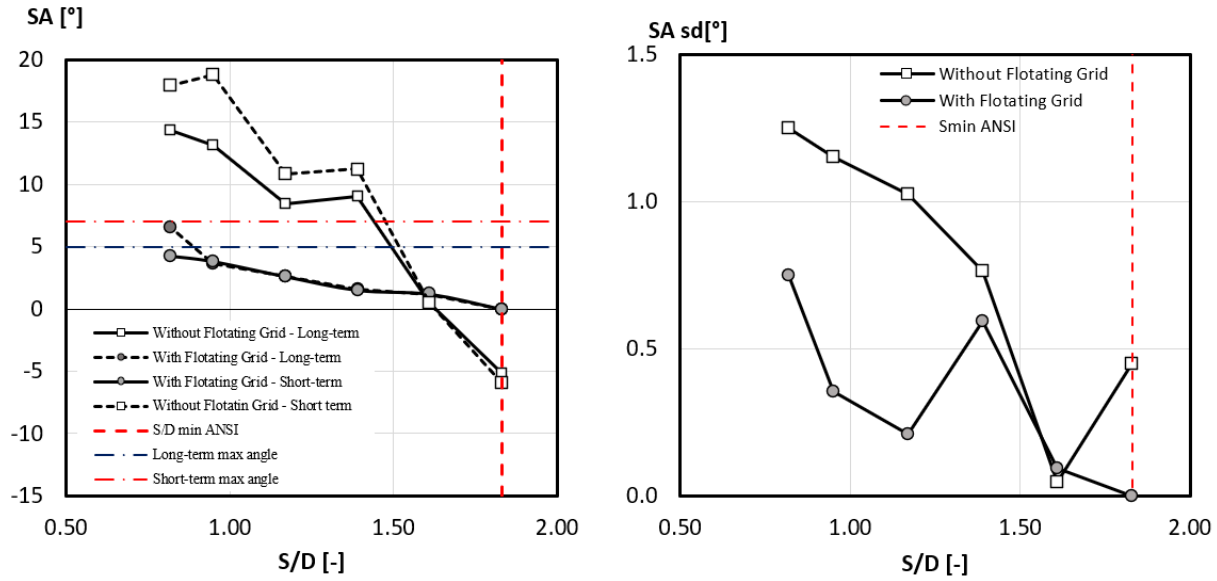

Figure 8. Swirl in the suction pipe, with and without the FG for a submergence level between 0.82 to 1.83 *S/D*. Left, Short-term, and the long-term average value of swirl angle. Without the FG, swirl angle values do not accomplish ANSI limits for *S/D* below 1.61. Right, Standard Deviation for swirl angle. Without the FG, swirl fluctuation is larger.

3.4. Flow visualization

Figure 9 shows an interpretation of superficial flow visualization for all the tested cases. Submergence levels of 1.39, 1.17, 0.95, and 0.82 as *S/D* ratios are included in the same scheme since they have the same superficial pattern. The main two differences for the cases with FG (Figure 9.b) are that the superficial vortices develop upstream of the FG, since the flow inside the grid cells has no movement and the vortices strength is much smaller for *S/D* < 1.61 (Table 3), and that the flow pattern as a function of submergence is the same with and without FG; for *S/D* = 1.83, the flow concentrates on the right side, the swirl is positive inside the suction pipe, and for superficial vortex. For *S/D* = 1.61 the flow and vortex formation are symmetric. Swirl inside the suction pipe is zero. For *S/D* < 1.39, the flow configuration is the opposite of *S/D* = 1.83, the flow concentrates on the left side and the swirl is negative inside the suction pipe and for the superficial vortex.

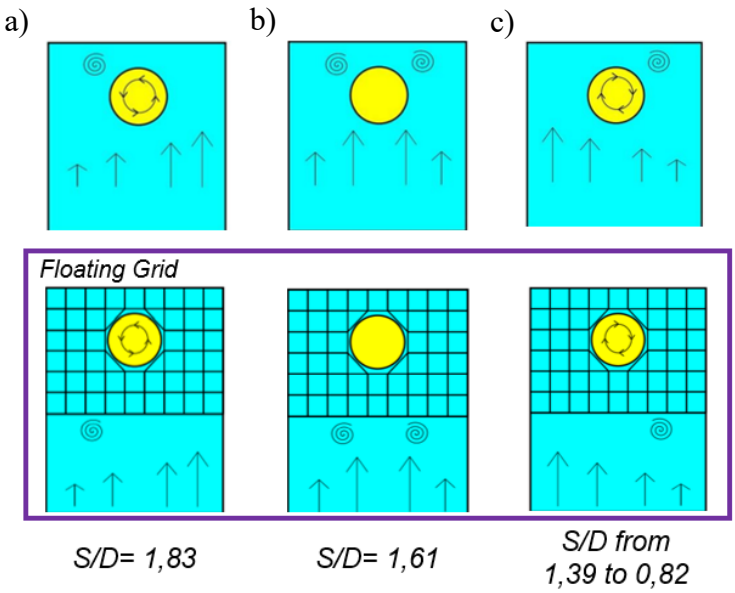

Figure 9 – Schematic interpretation of superficial flow visualization. a) Without FG: for *S/D* = 1.83, the flow concentrates on the right side and the swirl is positive inside the suction pipe and for the superficial vortex. For *S/D* = 1.61 the flow and vortex formation are symmetric. Swirl inside the suction pipe is zero. For *S/D* < 1.39, flow configuration is the opposite of *S/D* = 1.83. b) With FG: flow configuration remains the same as without FG for all the cases, superficial vortex location now is located upstream the FG.

Table 3. Vortex type characterization for every tested case according to ANSI standard (figure 3).

	Vortex type visualization					
Case	**1.83 S/D**	**1.61 S/D**	**1.39 S/D**	**1.17 S/D**	**0.95 S/D**	**0.82 S/D**
Without Floating Grid	T1	T1	T2	T3	T4	T5
With Floating Grid	T1	T1	T1	T1	T3	T4

4. Discussion and conclusions

Physical model tests were performed to evaluate the capability of the design named Floating Grid, to reduce vortex formation at the pump bay for a vertical submerged pump. The work aims to test the effectiveness of the device but not to optimize its geometry. Tests were carried out for a large flow of 1.3 times the design flow in order to achieve a conservative prediction. The design of the pump bay corresponds to a standard bay without fillets or splitter. The surface water level at the bay started from the minimum recommended by the pump designer (in coincidence with the ANSI code guidelines) *S/D* = 1.83, to a lower water level of *S/D* = 0.82, which can also be expressed as the 60 % of the minimum submergence.

Different techniques to quantify and describe the flow and the swirl formation were applied, such as PIV analysis, ADV velocity profiles, swirl angle measurements and vortex visualization and classification.

Based on these results, the most appropriate technique to evaluate the Floating Grid efficiency was the swirl angle measurements. The FG reduces the swirl angle at the entrance of the pump letting the same pump bay design achieve a swirl angle under 5° (as ANSI/HI code recommends) for an *S/D* = 0.82 instead of *S/D* = 1.83. The rest of the flow measurements prove that the flow with the presence of the FG is more stable, keeps vortices far from the suction bell and the pump case, and also reduces the vortices intensity, as shown in Table 3. Results have shown that the FG reduced the contribution of free surface vortices to the swirl angle as was expected, but part of the remaining circulation could be attributed to subsurface vortices.

Regarding the grid design, the minimum cell dimension to meet modular design guidelines would be 0.25 *D* x 0.25 *D*, but as it depends on the pump body diameter and the presence of bottom fillets, cell dimensions can be slightly adjusted to fit the bay geometry. A grid extending upstream will contribute to keeping upstream free surface far from

the suction bell, but it is not recommended to reduce this dimension. Also, a grid with smaller cell dimensions will help to reduce vortex intensity inside the cells, but a denser and longer grid will result in a more expensive solution.

It is expected that the efficiency of the grid will decline with higher flows so the 0.82 *S/D* submergence could not be achieved without a free vortex surface.

The key to good efficiency is that the FG can track the free surface level preventing big vortices from arising or grouping, and keeping them off the pump. Designers and pump station owners can implement this solution without the need to carry out a study on a physical model, as the main dimensions of the floating grid are indicated in this work.

Future work will focus on the comparison between different device designs and extend the test area to higher flows and lower levels.

5. ACKNOWLEDGMENTS

This work was possible with the collaboration of J. F. Varvasino and F. Balzacca both undergraduate students of Hydraulic Engineering and the support of Central Térmica Vuelta de Obligado company (CVOSA).

6. REFERENCES

ANSI/HI 9.8 (2018). American National Standard for Pump Intake Design, Hydraulic Institute, New Jersey.

Arocena, V.M., Abuan, B.E., Reyes, J.G.T., Rodgers, P.L and Danao, L.A.M. (2021) "Numerical investigation of the performance of a submersible pump: prediction of recirculation, vortex formation, and swirl resulting from off-design operating conditions." *Energies 2021*, 14, 5082.

Constantinescu G.S. and Patel, V.C. (1998). "Numerical model for simulation of pump-intake flow and vortices." *J. Hydraul. Eng.* 124:123-134.

Harun, Z. (2020). Vortex Dynamics Theories and Applications, IntechOpen, London.

Jones, G.M., Sanks, R.L., Tchobanoglous, G. and Bosserman, B.E. (2006). Pumping Station Design, Elsevier, USA.

Kushwaha, T.N. (2015). "CW pump fluid induced vibration troubleshooting methodology". *Procedia Engineering*, 144, 274-282.

Norizan, T.A., Harun, Z., Abdullah, S. and Mohtar, W.H. (2019). "Effects of floor splitter height on the effectiveness of swirl angle reduction in pump intake*." J. Adv. Res. Fluid Mech. Therm. Sci.,* 57, 1, 32-39.

Odgaard, J.A. (1986). "Free-surface air core Vortex". *J. Hydraul. Eng.*, 112(7), 610-620.

Park, I., Kim, H.-J., Seong, H. and Rhee, D.S. (2018). "Experimental studies on surface vortex mitigation using the floating anti-vortex device in sump pumps". *Water*, 10(4), 441.

Shrestha, U. and Choi, Y.-D. (2021). "Bellmouth shape optimization for the suppression of flow instability in a pump sump model." KSFM *J. Fluid Mach.*, 24(5), 49-57.

Taghvaei, S.M., Roshan, R., Safavi, K. and Sarkardeh, H. (2012). "Anti-vortex structures at hydropower dams." *Int. J. Phys. Sci.,* 7(28), 5069-5077.